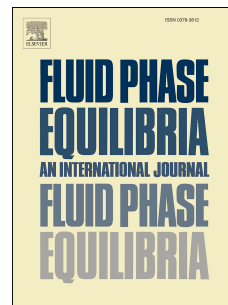


# Accepted Manuscript

Synthesis and characterization of analogues of glycine-betaine ionic liquids and their use in the formation of aqueous biphasic systems

Matheus M. Pereira, Sónia N. Pedro, Joana Gomes, Tânia E. Sintra, Sónia P.M. Ventura, João A.P. Coutinho, Mara G. Freire, Aminou Mohamadou



PII: S0378-3812(19)30203-1

DOI: <https://doi.org/10.1016/j.fluid.2019.05.001>

Reference: FLUID 12184

To appear in: *Fluid Phase Equilibria*

Received Date: 28 December 2018

Revised Date: 19 April 2019

Accepted Date: 2 May 2019

Please cite this article as: M.M. Pereira, Sónia N. Pedro, J. Gomes, Tânia E. Sintra, Sónia P.M. Ventura, João A.P. Coutinho, Mara G. Freire, Aminou Mohamadou, Synthesis and characterization of analogues of glycine-betaine ionic liquids and their use in the formation of aqueous biphasic systems, *Fluid Phase Equilibria* (2019), doi: <https://doi.org/10.1016/j.fluid.2019.05.001>.

This is a PDF file of an unedited manuscript that has been accepted for publication. As a service to our customers we are providing this early version of the manuscript. The manuscript will undergo copyediting, typesetting, and review of the resulting proof before it is published in its final form. Please note that during the production process errors may be discovered which could affect the content, and all legal disclaimers that apply to the journal pertain.

1 **Synthesis and characterization of analogues of glycine-betaine ionic liquids and**  
2 **their use in the formation of aqueous biphasic systems**

3  
4 **Matheus M. Pereira<sup>1</sup>, Sónia N. Pedro<sup>1</sup>, Joana Gomes<sup>1</sup>, Tânia E. Sintra<sup>1</sup>, Sónia P. M. Ventura<sup>1</sup>,**  
5 **João A. P. Coutinho<sup>1</sup>, Mara G. Freire<sup>1</sup>, Aminou Mohamadou<sup>2\*</sup>**

6  
7  
8 <sup>1</sup>CICECO – Aveiro Institute of Materials, Department of Chemistry, University of Aveiro, Campus  
9 Universitário de Santiago, 3810-193 Aveiro, Portugal

10 <sup>2</sup>Institut de Chimie Moléculaire de Reims (ICMR), UMR CNRS 7312, Université de Reims  
11 Champagne-Ardenne, Moulin de la Housse, BP 1039 – 51687 Reims cedex 2, France.

12  
13  
14  
15  
16 \* Corresponding author: Tel: +33 (0)32691 3334; Fax: +33 (0)32691 3243

17 E-Mail : [aminou.mohamadou@univ-reims.fr](mailto:aminou.mohamadou@univ-reims.fr) (A. Mohamadou)

22  
23 A series of novel analogues of glycine-betaine ionic liquids (AGB-ILs), viz. 1-(4-ethoxy-4-oxobutyl)-1-  
24 methylpyrrolidin-1-ium, N,N,N-tri(*n*-butyl)(4-ethoxy-4-oxobutyl)-1-phosphonium and N,N,N-  
25 trialkyl(4-ethoxy-4-oxobutyl)-1-aminium cations with ethyl, *n*-propyl and *n*-butyl alkyl chains,  
26 combined with the bromide anion, have been synthesized and characterized. Their synthesis and  
27 characterization by spectroscopic methods and elemental analysis is here reported. These ILs were  
28 further characterized in what concerns their thermal properties and ecotoxicity against *Allvibrio fischeri*,  
29 and compared with the commercial tetra(*n*-butyl)ammonium and tetra(*n*-butyl)phosphonium bromide.  
30 The novel AGB-ILs described in this work have low melting points, below 100 °C, display high  
31 degradation temperatures (180-310 °C), and low toxicity as shown by being harmless or practically  
32 harmless towards the marine bacteria *Allvibrio fischeri*. Finally, the ability of the synthesized AGB-ILs  
33 to form aqueous biphasic systems with potassium citrate/citric acid (at pH 7) was evaluated, and the  
34 respective ternary phase diagrams were determined. It is shown that the increase of the cation alkyl  
35 chain length facilitates the creation of ABS, and that phosphonium-based ILs present a slightly better  
36 separation performance in presence of aqueous solutions of the citrate-based salt.

37  
38  
39 *Key words:* Ionic liquids, analogues of glycine-betaine, thermal properties, ecotoxicity, *Allvibrio*  
40 *fischeri*, aqueous biphasic systems, phase diagram.

In order to replace volatile organic solvents, which may be harmful to both the process operators and the environment [1], many researchers have focused on the development of “greener solvents” [2]. Amongst these solvents, aprotic ionic liquids (ILs) are an interesting class of fluids since, if properly designed, they display a negligible vapour pressure at ambient conditions, non-flammability, high chemical and thermal stabilities, and unique solvation capabilities. As a result of these features, they have attracted attention as solvents for chemical and electrochemical reactions, biphasic catalysis, chemical syntheses, separation processes, among others [3-6]. Nevertheless, some ILs may display some toxicity and cause biodegradability concerns [7, 8]. Therefore, the design of more environmentally benign ILs has been a hot topic over the past years [9]. To obtain “greener” ILs, the starting materials should be non-toxic and renewable, and their synthesis environmentally-friendly [10]. The synthesis of ILs from renewable raw materials is more beneficial and attractive compared to the use of compounds derived from fossil feedstocks. In recent years, several bio-based ILs with biocompatible character have been synthesized and characterized, receiving considerable attention for distinct applications [11, 12]. Cholinium based-ILs emerged in several reports as biocompatible alternatives over the well-known imidazolium-based counterparts on the dissolution of biomass, CO<sub>2</sub> absorption processes or biomaterials development [13-15]. More recently, amino-acid- and carbohydrate-based ILs have been proposed to improve the biocompatible properties of ILs. The first have been tested in the pretreatment of lignocellulosic materials and as catalysts in organic synthesis [16-19], while the later have recently been proposed as novel chiral solvents [20, 21].

Previously, we reported the synthesis and characterization of ILs wherein the cation is either an alkyl ester glycine-betaine (GB) [22] or an analogue of glycine-betaine (AGB) [23], in which the ammonium cation comprises three alkyl groups and an ethyl acetate group. Hydrophobic GB-ILs have been applied in liquid-liquid extraction of pesticides [24], while AGB-ILs were employed in the extraction of metals from aqueous solutions [25-27]. On the other hand, hydrophilic (water-miscible) AGB-ILs have been used in the extraction of value-added compounds from biomass [28]. The cytotoxicity of these ILs aqueous solutions containing the biomass extracts was assessed in a macrophage cell line, as well as their anti-inflammatory potential via reduction of lipopolysaccharide-induced cellular oxidative stress, showing that the IL aqueous solutions enriched in the biomass extracts display higher antioxidant and anti-inflammatory effects than the recovered solid extracts, and that these solutions may be used in nutraceutical and cosmetic applications [28].

Glycine-betaine, which is a zwitterionic acetate group bearing a quaternary tri(methyl)ammonium, can be found in sugar beet molasses (up to 27 wt%) after the extraction of saccharose [29]. These organic osmolytes are recognized by their accumulation in a wide variety of plants in response against environmental stress. They have positive effects on enzyme and membrane

82 integrity along with adaptive roles in mediating osmotic adjustment in plants growing under stress  
 83 conditions [30, 31]. Furthermore, glycine-betaine and their derivatives are currently used as food  
 84 supplements [32], as well as in cosmetic lotions and formulations [33]. Given the benefits and “green”  
 85 credentials associated to glycine-betaine, we hereby report on the synthesis and characterization of 5  
 86 new bromide-based AGB-ILs, in which the cation carries an ethyl ester butyrate and three alkyl groups.  
 87 Two commercial ILs, namely tetrabutylammonium bromide and tetrabutylphosphonium bromide, were  
 88 also investigated for comparison purposes. The AGB-ILs synthesis and characterization are reported,  
 89 and their thermal properties, such as melting point, glass transition temperature and decomposition  
 90 temperature, were determined. The ecotoxicity of the synthesized AGB-ILs towards *Allvibrio fischeri*  
 91 was assessed using the Microtox<sup>®</sup> acute toxicity test [34, 35]. Finally, while envisaging their application  
 92 in separation processes, their ability to create aqueous biphasic systems (ABS) in presence of potassium  
 93 citrate was investigated.

94

## 95 2. Experimental Section

### 96 2.1. Materials

97 All used chemicals are described in Table 1, which comprises the CAS number, molecular  
 98 weight, purity and supplier.

99 **Table 1**

100 Name, CAS number, molecular weight, purity and supplier of the used chemicals.

Reagents	CAS number	Molecular weight	Purity (%)	Supplier
N-methylpyrrolidine	121-44-8	85.15	≥ 97	Sigma Aldrich
triethylamine	121-44-8	101.19	> 99	Fischer Scientific
tri( <i>n</i> -propyl)amine	102-69-2	143.27	≥ 98	Sigma Aldrich
tri( <i>n</i> -butyl)amine	102-82-9	185.35	≥ 98	Fischer Scientific
4-bromobutyric acid ethyl ester	2969-81-5	195.05	≥ 97	Sigma Aldrich
tripotassium citrate monohydrate	6100-05-6	324.42	≥ 99	Fischer Scientific
citric acid monohydrate·H <sub>2</sub> O	5949-29-1	210.14	100	Sigma Aldrich
tetrabutylammonium bromide	1643-19-2	322.37	> 97	Fluka
tetrabutylphosphonium bromide	3115-68-2	339.33	> 98	Sigma Aldrich

101

## 2.2. Synthesis of AGB-ILs

### 2.2.1. 1-(4-ethoxy-4-oxobutyl)-1-methylpyrrolidin-1-ium bromide ([MepyrNC<sub>4</sub>]Br · H<sub>2</sub>O)

A solution of 4-bromobutyrate acid ethyl ester (42.9 g, 0.22 mol) in ethyl acetate (100 mL) was added to a solution of N-methylpyrrolidine (29.8 g, 0.35 mol) in 110 mL of ethyl acetate. The mixture was stirred at room temperature for 24 days. The precipitate produced during the reaction was filtered, and washed twice with ethyl acetate and then with ethyl ether, and dried under vacuum. Yield (54.5 g, 83%). Elemental analysis: Found: C, 44.40; H, 7.80; N, 4.70%. Calculated for C<sub>11</sub>H<sub>24</sub>BrNO<sub>3</sub> (MW = 298.22 g·mol<sup>-1</sup>): C, 44.30; H, 8.11; N, 4.70%. <sup>1</sup>H NMR, δ/ppm (300 MHz, DMSO-*d*<sub>6</sub>): 1.20 [3 H, t, CH<sub>3</sub>(β)]; 2.01 [2 H, m, CH<sub>2</sub>(2)]; 2.08 (2 H, s, CH<sub>3</sub>(c)]; 2.41 [2 H, t, CH<sub>2</sub>(3)]; 3.38 [2 H, m, CH<sub>2</sub>(b)]; 3.56 (6 H, m, CH<sub>2</sub>(a+1)]; 4.09 (2 H, q, CH<sub>2</sub>(α)). <sup>13</sup>C NMR, δ/ppm (75.47 MHz, DMSO-*d*<sub>6</sub>): 11.2 [CH<sub>3</sub>(β)]; 14.8 [CH<sub>3</sub>(c)]; 19.1 [CH<sub>2</sub>(2)]; 21.7 [CH<sub>2</sub>(3)]; 23.0 [CH<sub>2</sub>(1)]; 31.3 [CH<sub>2</sub>(b)]; 56.9 3 [CH<sub>2</sub>(a)]; 60.5 [CH<sub>2</sub>(α)]; 172.5 [C=O(4)]. ESI-MS, m/z Found (Calculated): 200.16 (200.30) [C<sub>11</sub>H<sub>22</sub>NO<sub>2</sub><sup>+</sup>]; 115.07 (115.15) [C<sub>6</sub>H<sub>11</sub>O<sub>2</sub><sup>+</sup>]. IR (ν/cm<sup>-1</sup>): 3390 (ν<sub>O-H</sub>); 2955, 2870 (ν<sub>C-H</sub>); 1720 (ν<sub>C=O</sub>); 1286 (ν<sub>C-N</sub>).

### 2.2.2. N,N,N-tri(*n*-alkyl)(4-ethoxy-4-oxobutyl)-1-aminium bromide

Tri(ethyl)[4-ethoxy-4-oxobutyl]ammonium bromide and Tri(*n*-propyl)[4-ethoxy-4-oxobutyl]ammonium bromide were synthesized as described for (N-methylpyrrolidyl-4-ethoxy-4-oxobutyl)ammonium bromide using tri(ethyl)amine (35.4 g, 0.35 mol) and tri(*n*-propyl)amine (50.1 g, 0.35 mol), respectively.

#### 2.2.2.1. N,N,N-tri(ethyl)(4-ethoxy-4-oxobutyl)-1-aminium bromide ([Et<sub>3</sub>NC<sub>4</sub>]Br · 0.2 H<sub>2</sub>O)

Yield (52.8 g, 80%). Elemental analysis: Found: C, 48.00; H, 8.90; N, 4.50%. Calculated for C<sub>12</sub>H<sub>24.4</sub>BrNO<sub>2.2</sub> (MW = 299.85 g·mol<sup>-1</sup>): C, 48.07; H, 8.87; N, 4.67%. <sup>1</sup>H NMR, δ/ppm (300 MHz, DMSO-*d*<sub>6</sub>): 1.19 [12 H, m, CH<sub>3</sub>(β+b)]; 1.88 [2 H, m, CH<sub>2</sub>(2)]; 2.45 [2 H, t, H<sub>2</sub>(3)]; 3.15 [2 H, t, CH<sub>2</sub>(1)]; 3.24 [6H, q, CH<sub>2</sub>(a)]; 4.08 [2 H, q, CH<sub>2</sub>(α)]. <sup>13</sup>C NMR, δ/ppm (75.47 MHz, DMSO-*d*<sub>6</sub>): δ 14.1 [CH<sub>3</sub>(b)]; 19.6 [CH<sub>3</sub>(β)]; 23.5 [CH<sub>2</sub>(2)]; 58.0 [CH<sub>2</sub>(a)], 60.7 [CH<sub>2</sub>(1)]; 62.7 [CH<sub>2</sub>(α)]; 172.4 [C=O(4)]. ESI-MS, m/z Found (Calculated): 216.1<sub>-</sub> (216.34) [C<sub>12</sub>H<sub>26</sub>NO<sub>2</sub><sup>+</sup>]; 115.08 (115.15) [C<sub>6</sub>H<sub>11</sub>O<sub>2</sub><sup>+</sup>] IR (ν/cm<sup>-1</sup>): 3400 (ν<sub>O-H</sub>); 2950, 2865 (ν<sub>C-H</sub>); 1725 (ν<sub>C=O</sub>); 1280 (ν<sub>C-N</sub>).

#### 2.2.2.2. N,N,N-tri(*n*-propyl)(4-ethoxy-4-oxobutyl)-1-aminium bromide ([Pr<sub>3</sub>NC<sub>4</sub>]Br · 0.7 H<sub>2</sub>O)

Yield (62.5 g, 81%). Elemental analysis: Found: C, 51.50; H, 9.60; N, 4.20%. Calculated for C<sub>15</sub>H<sub>33.4</sub>BrNO<sub>2.7</sub> (MW = 350.94 g·mol<sup>-1</sup>): C, 51.34; H, 9.59; N, 3.99%. <sup>1</sup>H NMR, δ/ppm (300 MHz, DMSO-*d*<sub>6</sub>): 0.90 [9 H, t, CH<sub>3</sub>(c)]; 1.20 [3 H, t, CH<sub>3</sub>(β)]; 1.65 [6 H, m, CH<sub>2</sub>(b)]; 1.81 [2 H, m, CH<sub>2</sub>(2)]; 2.43 [2 H, t, CH<sub>2</sub>(3)]; 3.20 (8 H, m, CH<sub>2</sub>(a+1)]; 4.08 (2 H, q, CH<sub>2</sub>(α)). <sup>13</sup>C NMR, δ/ppm (75.47 MHz,

136 DMSO-*d*<sub>6</sub>): 11.1 [CH<sub>3</sub>(c)]; 14.4 [CH<sub>3</sub>(β)]; 15.2 [CH<sub>2</sub>(b)]; 16.8 [CH<sub>2</sub>(2)]; 30.1 [CH<sub>2</sub>(3)]; 59.7  
137 [CH<sub>2</sub>(a+1)]; 60.7 [CH<sub>2</sub>(α)]; 172.4 [C=O(4)]. ESI-MS, m/z Found (Calculated): 258.24 (258.42)  
138 [C<sub>15</sub>H<sub>32</sub>NO<sub>2</sub><sup>+</sup>]; 115,08 (115,15) [C<sub>6</sub>H<sub>11</sub>O<sub>2</sub><sup>+</sup>] IR (v/cm<sup>-1</sup>): 3450 (ν<sub>O-H</sub>); 2957, 2866 (ν<sub>C-H</sub>); 1728 (ν<sub>C=O</sub>);  
139 1285 (ν<sub>C-N</sub>).

140

### 141 2.2.3. N,N,N-tri(*n*-butyl)(4-ethoxy-4-oxobutyl)-1-aminium bromide ([Bu<sub>3</sub>NC<sub>4</sub>]Br)

142 To tri(*n*-butyl)amine (68.9 g, 0.35 mol) in 110 mL of ethyl acetate, it was added (42.9 g, 0.22 mol) 4-  
143 bromobutyrate acid in 100 mL of ethyl ester, under stirring. The mixture was refluxed for 48h and then  
144 stirred at room temperature for 2h. The solution separates into two phases, and the bottom phase  
145 corresponding to the brownish oil was recovered, and washed three times with 100 mL of ethyl acetate,  
146 and then kept in the freezer for 48 h. The white product, which crystallized after 48 hours, was  
147 successively washed with ethyl acetate and diethyl ether, and then dried under vacuum. Yield (71.1 g,  
148 85%). Elemental analysis: Found: C, 57.04; H, 9.90; N, 3.50%. Calculated for C<sub>18</sub>H<sub>38</sub>BrNO<sub>2</sub> (MW =  
149 380.41 g·mol<sup>-1</sup>): C, 56.83; H, 10.07; N, 3.68%. <sup>1</sup>H NMR (300 MHz, DMSO-*d*<sub>6</sub>): 0.94 [9 H, t, CH<sub>3</sub>(d)];  
150 1.21 [3 H, t, CH<sub>3</sub>(β)]; 1.37 [6 H, m, CH<sub>2</sub>(c)]; 1.64 [6 H, m, CH<sub>2</sub>(b)]; 1.89 [2 H, m, CH<sub>2</sub>(2)]; 2.43 [2 H, t,  
151 CH<sub>2</sub>(3)]; 3.21 [8 H, m, CH<sub>2</sub>(a+1)]; 4.09 [2 H, q, CH<sub>2</sub>(α)]. <sup>13</sup>C NMR, δ/ppm (75.47 MHz, DMSO-*d*<sub>6</sub>):  
152 14.1 [CH<sub>3</sub>(d)]; 19.6 [CH<sub>3</sub>(β)], 23.5 [CH<sub>3</sub>(c)]; 33.1 [CH<sub>2</sub>(2)]; 56.8 [CH<sub>2</sub>(b)]; 58.0 [CH<sub>2</sub>(3)]; 60.7  
153 [CH<sub>2</sub>(1+a)]; 62.7 [CH<sub>2</sub>(α)]; 172.2 [C=O(4)]. ESI-MS, m/z Found (Calculated): 300.27 (300.50)  
154 [C<sub>18</sub>H<sub>38</sub>NO<sub>2</sub><sup>+</sup>]; 115.08 (115.15) [C<sub>6</sub>H<sub>11</sub>O<sub>2</sub><sup>+</sup>] IR (v/cm<sup>-1</sup>): 2960, 2872 (ν<sub>C-H</sub>); 1728 (ν<sub>C=O</sub>); 1283 (ν<sub>C-N</sub>).

155

### 156 2.2.4. Tri(*n*-butyl)(4-ethoxy-4-oxobutyl)-1-phosphonium bromide ([Bu<sub>3</sub>PC<sub>4</sub>]Br)

157 Tri(*n*-butyl)[4-ethoxy-4-oxobutyl]phosphonium bromide was synthesized as described for N,N,N-tri(*n*-  
158 butyl)(4-ethoxy-4-oxobutyl)-1-aminium bromide using tri(*n*-butyl)phosphine (65.2 g, 0.35 mol) as  
159 amine. Yield (73.4 g, 84%). Elemental analysis: Found: C, 54.36; H, 9.85%. Calculated for  
160 C<sub>18</sub>H<sub>38</sub>BrPO<sub>2</sub> (MW = 397.37 g·mol<sup>-1</sup>): C, 54.42; H, 9.58%. <sup>1</sup>H NMR (300 MHz, DMSO-*d*<sub>6</sub>): 0.90 [9H, t,  
161 CH<sub>3</sub>(d)]; 1.24 [3H, t, CH<sub>3</sub>(β)]; 1.40 [12H, m, CH<sub>2</sub>(b+c)]; 1.76 [2H, m, CH<sub>2</sub>(2)]; 2.25 [8H, m, CH<sub>2</sub>(a+1)];  
162 2.50 [2H, m, CH<sub>2</sub>(3)]; 4.10 [2H, q, CH<sub>2</sub>(α)]. <sup>13</sup>C NMR, δ/ppm (75,47 MHz, DMSO-*d*<sub>6</sub>): 13.3 [CH<sub>3</sub>(d)];  
163 14.1 [CH<sub>3</sub>(β)]; 23.4 [CH<sub>2</sub>(c)]; 23.7 [CH<sub>2</sub>(b)];, 33.6, [CH<sub>2</sub>(2)]; 58.0 [CH<sub>2</sub>(3)]; 60.6 [CH<sub>2</sub>(1+a)]; 62.7  
164 [CH<sub>2</sub>(α)]; 169.1 (C=O(4)). ESI-MS, m/z Found (Calculated): 317.25 (317.47) [C<sub>18</sub>H<sub>38</sub>PO<sub>2</sub><sup>+</sup>]; 259.24  
165 (259.97) [C<sub>11</sub>H<sub>29</sub>PO<sub>2</sub><sup>+</sup>]. IR (v/cm<sup>-1</sup>): 2960, 2928, 2874 (ν<sub>C-H</sub>); 1727 (ν<sub>C=O</sub>); 1233 (ν<sub>C-N</sub>).

166

167 The full name, abbreviation and chemical structure of the synthesized AGB-ILs are summarized in  
168 Table 2.

169

170  
171  
172  
173

**Table 2.**

Name, abbreviation, chemical structure and molecular weight of the synthesized AGB-ILs, and of two commercial ILs investigated for comparison purposes.

Name	Abbreviation	Chemical Structure and Atoms Identification	Molecular Weight (g.mol <sup>-1</sup> )
1-(4-ethoxy-4-oxobutyl)-1-methylpyrrolidin-1-ium bromide	[MepyrNC <sub>4</sub> ]Br		280.22
N,N,N-triethyl(4-ethoxy-4-oxobutyl)-1-aminium bromide	[Et <sub>3</sub> NC <sub>4</sub> ]Br		296.25
N,N,N-tri( <i>n</i> -propyl)(4-ethoxy-4-oxobutyl)-1-aminium bromide	[Pr <sub>3</sub> NC <sub>4</sub> ]Br		338.33
N,N,N-tri( <i>n</i> -butyl)(4-ethoxy-4-oxobutyl)-1-aminium bromide	[Bu <sub>3</sub> NC <sub>4</sub> ]Br		380.41
Tri( <i>n</i> -butyl)(4-ethoxy-4-oxobutyl)-1-phosphonium bromide	[Bu <sub>3</sub> PC <sub>4</sub> ]Br		397.37
Tetra( <i>n</i> -butyl)ammonium bromide	[N <sub>4444</sub> ]Br		324.41
Tetra( <i>n</i> -butyl)phosphonium bromide	[P <sub>4444</sub> ]Br		341.37

174  
175



All IL samples were dried under vacuum (10 Pa) at room temperature for a minimum of 48h before carrying out their characterization. The water content of the dried ILs was determined by Karl Fischer coulometry using a Metrohm 787 KF Titrino coulometer with Hydranal 34805 and Hydranal 37817 (from Fluka) as titrant; their water concentration was less than  $6 \times 10^{-4}$  in weight fraction. During the preparation of the ILs aqueous solutions for the ecotoxicity assays and ternary phase diagrams determination, the water content of each IL was taken into account. Elemental analyses (C, H, N and S contents) of all synthesized ILs were carried on a Perkin-Elmer 2400 C, H, N and S element analyzer. Infra-Red (IR) spectra were recorded at room temperature with a PerkinElmer UATR Two spectrometer.  $^1\text{H}$  and  $^{13}\text{C}$  Nuclear magnetic resonance (NMR) were recorded at room temperature with a Bruker AC 30 spectrometer (250 MHz for  $^1\text{H}$ , 62.5 MHz for  $^{13}\text{C}$ ) using  $\text{DMSO-}d_6$  as solvent. Chemical shifts (in ppm) for  $^1\text{H}$  and  $^{13}\text{C}$  NMR spectra are referenced to residual protic solvent peaks. Electrospray ionization mass spectrometry (ESI-MS) of AGB-ILs diluted in methanol were obtained on a hybrid tandem quadrupole/time-of-flight (Q-TOF) instrument, equipped with a pneumatically assisted electrospray (Z-spray) ion source (Micromass, Manchester, UK) operated in positive mode; the capillary voltage was 3500 V; and the extraction cone voltage varied between 30-60V with the flow of injection of 5 mL/min. The decomposition temperatures of the ILs were determined by thermogravimetric analyses (TGA) using a Netzsch TG 209 F3 Tarsus thermogravimetric analyzer, under nitrogen atmosphere, with samples of 10-20 mg. These were heated from 30 °C to 500 °C, with a heating rate of 10 °C·min<sup>-1</sup>. Differential Scanning Calorimetry (DSC) experiments were performed with a TA Instruments Q100, under nitrogen atmosphere, with a cooling and heating rate of 10 °C·min<sup>-1</sup>.

#### 2.4. Microtox<sup>®</sup> acute toxicity tests

To address the ecotoxicity of the synthesized AGB-ILs, the standard Microtox<sup>®</sup> liquid-phase assay [36] was used, in which it is evaluated the luminescence inhibition of the bacteria *Allvibrio fischeri* (strain NRRL B-11177) [37]. In this work, the standard 81.9% test protocol was followed [38]. The microorganism was exposed to a range of diluted aqueous solutions of each IL (from 0 to 81.9 wt%), where 100% of AGB-IL corresponds to a known concentration of a stock solution previously prepared [39]. After 5, 15 and 30 min of exposure of the bacterium to each IL aqueous solutions, the light output of the bacterium was assessed and compared with the light output of the blank control (an aqueous solution without AGB-ILs), enabling the calculation of the EC<sub>50</sub> values at 5, 15 and 30 min through the Microtox<sup>®</sup> Omni™ Software [39].

#### 2.5. ABS phase diagrams

Aqueous solutions of each IL ( $[\text{MepyrNC}_4]\text{Br}$ ,  $[\text{Et}_3\text{NC}_4]\text{Br}$ ,  $[\text{Pr}_3\text{NC}_4]\text{Br}$ ,  $[\text{Bu}_3\text{NC}_4]\text{Br}$ ,  $[\text{Bu}_3\text{PC}_4]\text{Br}$ ) at

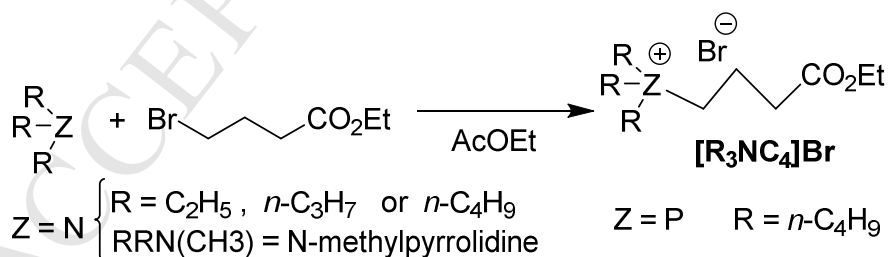
211 *circa* 70-90 wt% and aqueous solutions of the mixture  $K_3C_6H_5O_7/C_6H_8O_7$  (as a buffer solution at pH =  
 212 7.0, mole ratio of  $\approx 15:1$ ) at  $\approx 50$  wt% were prepared and used for the determination of the binodal  
 213 curves. The phase diagrams were determined through the cloud point titration method [40, 41] at  $(25 \pm$   
 214  $1)$  °C and atmospheric pressure. The system compositions were determined by the weight quantification  
 215 of all components added within  $\pm 10^{-4}$  g. Further details on the experimental procedure can be found  
 216 elsewhere [41, 42]. Tie-lines (TLs) and tie-line lengths (TLLs) were determined by a gravimetric  
 217 method originally described by Merchuk et al. [43].

218

### 219 3. Results and discussion

#### 220 3.1. AGB-ILs synthesis and characterization

221 Analogues of glycine-betaine ionic liquids (AGB-ILs) were obtained by the reaction of the  
 222 corresponding tertiary amine and 2-bromoacetic acid ethyl ester (Figure 1). GB-ILs were obtained at  
 223 yields higher than 80 %, and isolated and recovered as white solids at room temperature.  $^1H$  and  $^{13}C$   
 224 NMR spectra revealed the absence of organic impurities in the purified ILs. The electrospray ionization  
 225 mass spectra of the synthesized ILs are given in Figures S1 to S5 in the Supporting Information,  
 226 showing the presence of the organic cations  $[MeprNC_4^+]$  ( $m/z = 200.16$ ),  $[Et_3NC_4^+]$  ( $m/z = 216.18$ ),  
 227  $[Pr_3NC_4^+]$  ( $m/z = 258.24$ ),  $[Bu_3NC_4^+]$  ( $m/z = 300.27$ ) and  $[Bu_3PC_4^+]$  ( $m/z = 317.25$ ). The IR spectra of  
 228 all ILs show only weak absorption bands in the  $3000-3100\text{ cm}^{-1}$  region, indicating that the interaction  
 229 between the cation and anion of the ILs *via* hydrogen bonds is rather limited, a result of the bulky and  
 230 organic tetraalkylammonium and phosphonium cations. Therefore, it is mainly the cation-anion  
 231 coulombic attraction that ensures the cohesion of these salts. In addition, IR spectra for AGB-ILs  
 232 indicate the presence of water, according to the band in the  $3400\text{ cm}^{-1}$  region corresponding to OH  
 233 stretching.



234

235

236

**Fig. 1.** Synthetic route of AGB-ILs.

237 The data corresponding to the AGB-ILs melting point ( $T_m$ ), glass transition temperature ( $T_g$ ) and  
 238 decomposition temperature ( $T_{dec}$ ) corresponding to 10% of weight loss are given in Table 3. Melting  
 239 points were identified for all ILs, but no glass transition temperature ( $T_g$ ) has been observed for  
 240  $[Pr_3NC_4]Br$  and  $[Bu_3PC_4]Br$ . The DSC results of all the synthesized salts  $[R_3NC_4]Br$  ( $R_3N = N$ -  
 241 methylpyrrolidinyl or  $R =$  ethyl,  $n$ -propyl,  $n$ -butyl) are given in Figure S6 in the Supporting

242 Information. All the synthesized ILs have melting points below 100 °C, i.e. from 73 to 90 °C, which is  
 243 attributed to the bulky and asymmetric cation with high charge dispersion, and thus to the poor cation-  
 244 anion interactions. Furthermore, the melting points slightly increase with the alkyl chain at the cation, in  
 245 agreement with the literature [44]. On the other hand, [Bu<sub>3</sub>PC<sub>4</sub>]Br (T<sub>m</sub> = 88 °C) shows a lower melting  
 246 point than the corresponding ammonium salt [Bu<sub>3</sub>NC<sub>4</sub>][Br] (T<sub>m</sub> = 90 °C). The same behaviour, observed  
 247 with other ammonium- and phosphonium-based ILs including the commercial ones ([N<sub>4444</sub>][Br] with T<sub>m</sub>  
 248 = 104 °C and [P<sub>4444</sub>][Br] with T<sub>m</sub> = 101 °C), was attributed to the larger radius of the phosphorus atom  
 249 leading to a higher dispersion of charge [45]. It is known that the glass transition temperature is  
 250 approximately two-thirds of the melting point value [46]. The range of experimental T<sub>g</sub>/T<sub>m</sub> ratio was  
 251 found to be between 0.58 and 0.78 for different molecules and polymers [47]. The T<sub>g</sub>/T<sub>m</sub> of the prepared  
 252 ILs (given in Table 3) ranges between 0.64 and 0.72, fitting within the range of values reported in the  
 253 literature [47].

254

255 **Table 3**

256 Melting (T<sub>m</sub>), glass transition (T<sub>g</sub>) and decomposition (T<sub>dec</sub>) temperatures for the synthesized AGB-ILs.

257

AGB-ILs	T <sub>m</sub> (°C) <sup>a</sup>	T <sub>g</sub> (°C)	T <sub>g</sub> /T <sub>m</sub>	T <sub>dec</sub> (°C)
[MepyrNC <sub>4</sub> ]Br	73	-31	0.70	179
[Et <sub>3</sub> NC <sub>4</sub> ]Br	78	-21	0.72	187
[Pr <sub>3</sub> NC <sub>4</sub> ]Br	79	-	-	184
[Bu <sub>3</sub> NC <sub>4</sub> ]Br	90	-40	0.64	198
[Bu <sub>3</sub> PC <sub>4</sub> ]Br	88	-	-	310

263

264

265

(a) The uncertainty in the measured temperature was (± 0.2 °C).

266

267

268

269

270

271

272

273

274

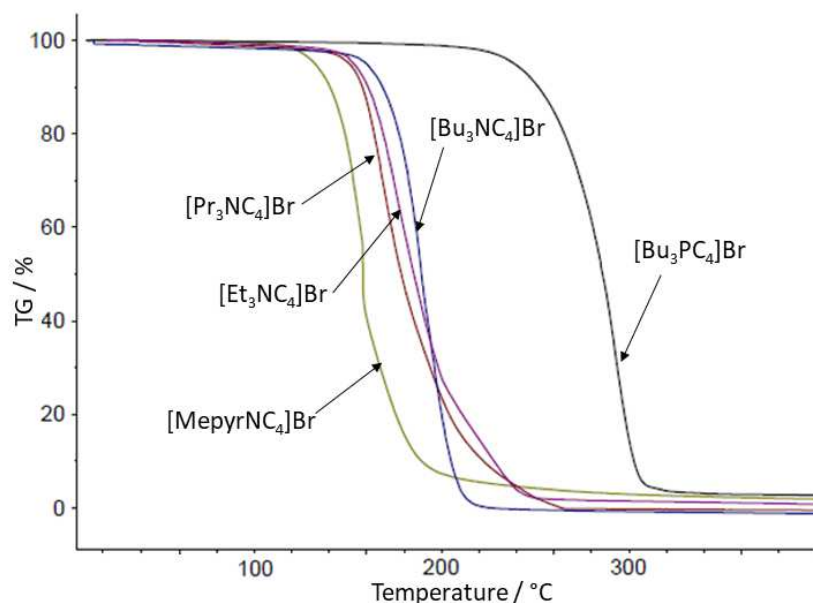
275

276

277

The thermal stability of the synthesized AGB-ILs was determined by TGA over the temperature range between 30 and 400 °C, being the respective data given in Table 3. The thermal degradation profile of the investigated ILs is shown in Figure 2, where the decomposition temperature (T<sub>dec</sub>) of all these salts falls in the range between 180 and 310 °C (Figure 2). The ILs thermal stabilities increase in the order: [MepyrNC<sub>4</sub>]Br < [Pr<sub>3</sub>NC<sub>4</sub>]Br < [Et<sub>3</sub>NC<sub>4</sub>]Br < [Bu<sub>3</sub>NC<sub>4</sub>]Br << [Bu<sub>3</sub>PC<sub>4</sub>]Br. With the exception of [Pr<sub>3</sub>NC<sub>4</sub>]Br IL (T<sub>dec</sub> = 184 °C), a slight increase in the thermal stability is observed when increasing the cation alkyl chain length. In addition, the cyclic ammonium [MepyrNC<sub>4</sub>]Br is the IL with the lowest T<sub>dec</sub> confirming that the thermal stability of these ILs mostly depends on the number of carbon atoms at the cation. For the ILs comprising ammonium cations, the maximum degradation temperature is obtained with the *n*-butyl groups. Furthermore, the tri(*n*-butyl)phosphonium-based IL is more thermally stable than the respective ammonium counterpart ([Bu<sub>3</sub>NC<sub>4</sub>]Br with T<sub>dec</sub> = 198 °C versus [Bu<sub>3</sub>PC<sub>4</sub>]Br with T<sub>dec</sub> = 310 °C). These results are in agreement with those of other

278 ammonium/phosphonium-based ILs, where phosphonium-based ILs present higher values of  $T_{dec}$  [48,  
279 49]. Tsunashima *et al.* [50] attributed this increase to the presence of empty d-orbitals on the  
280 phosphorus atom.  
281



282  
283 **Fig. 2.** TGA profiles for bromide based AGB-ILs.  
284

285 The five AGB-ILs were tested in terms of their effect against the marine luminescent bacteria *Allvibrio*  
286 *fischeri*. The  $EC_{50}$  values determined after 5, 15 and 30 min of exposure, and the respective 95%  
287 confidence limits, are reported in Table 4. The  $EC_{50}$  data at 30 min were adopted to ensure enough  
288 exposition time to verify the full effect in the luminescence inhibition [51]. The  $EC_{50}$  values at the same  
289 times of exposure for the commercial tetrabutylammonium and tetrabutylphosphonium bromide ILs  
290 ( $[N_{4444}]Br$ ,  $[P_{4444}]Br$ ) [52] are also displayed in Table 4 for comparison purposes. The higher the  $EC_{50}$   
291 values the less toxic is the IL towards this luminescent marine bacteria. Regardless of the exposure  
292 time, the results obtained show that the toxicity of AGB-ILs toward the bacteria increase according to  
293 the following sequence:  $[MepyrNC_4]Br < [Et_3NC_4]Br < [Pr_3NC_4]Br < [Bu_3NC_4]Br \ll [Bu_3PC_4]Br$ .  
294 Because all AGB-ILs share the bromide anion, the differences in their toxicity are a result of the IL  
295 cation. For the ammonium-based ILs, the toxicity increases with the alkyl chain length increase, being  
296 this a well-known trend recurrently named as the “side-chain effect” [53, 54]. The increase of the cation  
297 alkyl chain length leads to an increase of its hydrophobicity/lipophilicity, resulting in a higher ability to  
298 interact with and/or permeate phospholipid bilayers. Taking into account the cation central atom, the  
299  $EC_{50}$  values decrease from  $[Bu_3NC_4]Br$  to  $[Bu_3PC_4]Br$ , meaning that the ammonium-based IL is less  
300 toxic than its phosphonium-based counterpart, being in agreement with previous findings [55]. The  
301 same behavior is shown for the commercial ILs ( $[N_{4444}]Br$  vs.  $[P_{4444}]Br$ ). In general, all AGB-ILs  
302 synthesized and proposed in this work display a lower toxicity to *Allvibrio fischeri* than those

303 commonly used, namely [N<sub>4444</sub>]Br and [P<sub>4444</sub>]Br. All the studied AGB-ILs can be considered as  
 304 harmless or practically harmless (at 30 min of exposure:  $191 \text{ mg.L}^{-1} \leq \text{EC}_{50} \leq 3052 \text{ mg.L}^{-1}$ ) according to  
 305 Passino and Smith classification [56].

306 **Table 4**

307 Microtox<sup>®</sup> EC<sub>50</sub> values (mg.L<sup>-1</sup>) for *Allvibrio fischeri* after 5, 15 and 30 min of exposure to aqueous  
 308 solutions of AGB-ILs and of two commercial ILs [51, 52] with the respective 95% confidence limits (in  
 309 brackets).

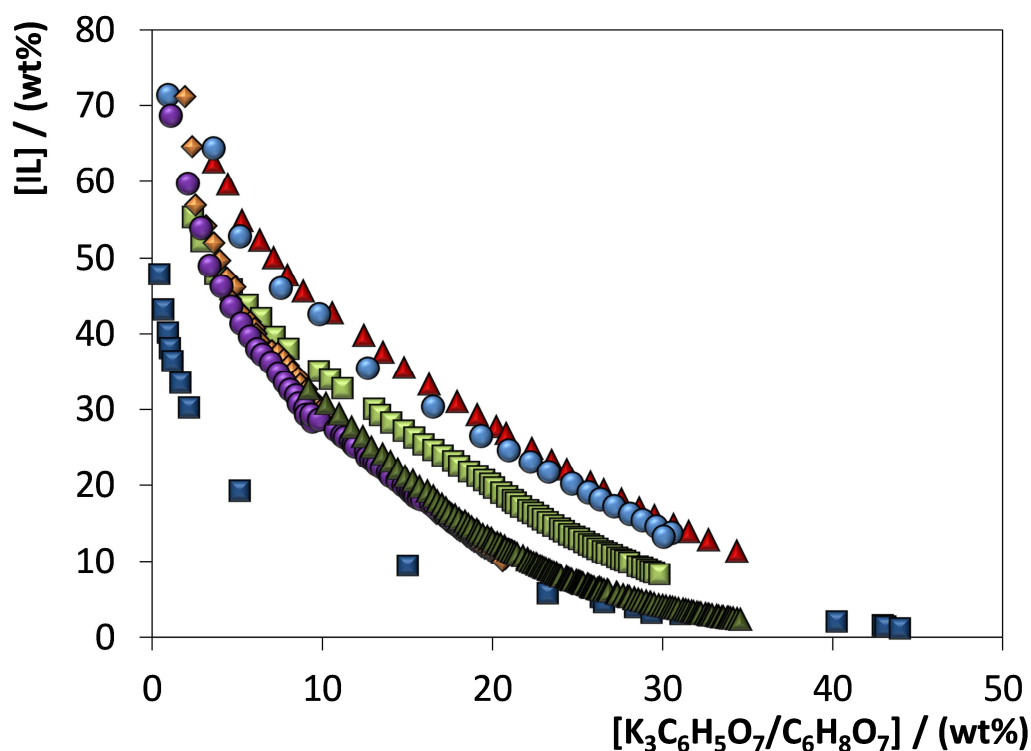
AGB-ILs	EC <sub>50</sub> (mg.L <sup>-1</sup> ) (lower limit; upper limit)		
	5 min	15 min	30 min
[MePyrNC <sub>4</sub> ]Br	3058.56 (1596.73; 4478.39)	3052.29 (2277.68; 4526.90)	3052.32 (1882.86; 4281.78)
[Et <sub>3</sub> NC <sub>4</sub> ]Br	2664.15 (1917.81; 3410.5)	2491.05 (1627.56; 3354.54)	2415.00 (1621.30; 3208.70)
[Pr <sub>3</sub> NC <sub>4</sub> ]Br	2157.05 (1678.50; 2635.61)	2026.41 (1411.48; 2641.35)	2018.72 (1267.08; 3630.37)
[Bu <sub>3</sub> NC <sub>4</sub> ]Br	435.43 (295.60; 575.27)	380.92 (260.06; 501.78)	327.22 (317.22; 336.78)
[Bu <sub>3</sub> PC <sub>4</sub> ]Br	351.76 (248.71; 454.83)	243.95 (239.41; 370.06)	191.30 (141.25; 200.45)
[N <sub>4444</sub> ]Br	233.30 (223.36; 243.15)	160.22 (143.55; 176.87)	-
[P <sub>4444</sub> ]Br	216.00 (21.60; 1382.40)	172.80 (0.00; 3218.40)	-

311  
312

### 313 3.2. ABS phase diagrams

314 The novel AGB-ILs proposed in this work have low melting points, below 100 °C, display high  
 315 degradation temperatures (180-310 °C), and low toxicity as shown by being harmless or practically  
 316 harmless towards the marine bacteria *Allvibrio fischeri*. Therefore, their use in a wide range of  
 317 applications can be envisioned. Aiming at exploring their use in liquid-liquid separation processes, we  
 318 addressed here their potential to form ABS with salts. Novel ternary phase diagrams were determined  
 319 for all the AGB-ILs + water + potassium citrate/citric acid mixtures (K<sub>3</sub>C<sub>6</sub>H<sub>5</sub>O<sub>7</sub>/C<sub>6</sub>H<sub>8</sub>O<sub>7</sub> mixtures, pH =  
 320 7.0) at 25°C and atmospheric pressure. In the respective phase diagrams, illustrated in Figure 3, the  
 321 biphasic region is localized above the solubility curve described by the experimental solubility data  
 322 points. Diagrams with a larger area above the binodal curve have therefore a higher ability to form two  
 323 phases, i.e. the IL is more easily salted-out by the citrate-based salt [57]. For comparison purposes, the  
 324 ternary phase diagrams for the commercial [N<sub>4444</sub>]Br and [P<sub>4444</sub>]Br under the same conditions, which  
 325 were previously reported [51, 52], are also provided. The corresponding experimental weight fraction  
 326 data are given in the Tables S1-S5 in the Supporting Information. All the calculations considering the

327 weight fraction of the phase-forming components were performed discounting the complexed water in  
328 the commercial citrate-based salt and citric acid.



329  
330

331 **Fig. 3.** Ternary phase diagrams, in an orthogonal representation, for the systems composed of IL +  
332 water +  $K_3C_6H_5O_7/C_6H_8O_7$  buffered at pH = 7.0 and at 25°C: [MepyrNC<sub>4</sub>]Br (▲); [EtNC<sub>4</sub>]Br (●);  
333 [PrNC<sub>4</sub>]Br (■); [BuNC<sub>4</sub>]Br (◆); [Bu<sub>3</sub>PC<sub>4</sub>]Br (●), [N<sub>4444</sub>]Br (▲) [57]; [P<sub>4444</sub>]Br (■) [58].

334 The phase diagrams shown in Figure 3 allow the evaluation of the effect of the ammonium alkyl  
335 chain length, the effect of the IL central atom (N vs. P), and the presence of cyclic cation structures  
336 against linear alkyl side chains. All studied compounds comprise the bromide anion, being the  
337 difference in liquid-liquid demixing a result of the IL cation nature. The capacity of AGB-ILs to form  
338 ABS (or to be salted-out by the organic citrate-based salt) follows the order: [Bu<sub>3</sub>PC<sub>4</sub>]Br > [Bu<sub>3</sub>NC<sub>4</sub>]Br  
339 > [Pr<sub>3</sub>NC<sub>4</sub>]Br > [Et<sub>3</sub>NC<sub>4</sub>]Br ≈ [MepyrNC<sub>4</sub>]Br. It is shown that the increase of the cation alkyl chain  
340 length facilitates the creation of ABS, meaning that longer alkyl side chain ILs are more easily salted-  
341 out by the organic salt, in agreement with literature data and demonstrating that this behavior is  
342 independent of the salt used [59-61]. On the other hand, [MepyrNC<sub>4</sub>]Br is the IL with the lowest ability  
343 to create ABS, as result of its higher hydrophilicity afforded by a lower number of methylene groups.  
344 The phase diagrams for the systems composed of [Bu<sub>3</sub>NC<sub>4</sub>]Br and [Bu<sub>3</sub>PC<sub>4</sub>]Br are also presented in  
345 Figure 3, allowing to appraise the effect of the IL cation central atom. Although with a similar chemical  
346 structure, [Bu<sub>3</sub>PC<sub>4</sub>]Br presents a slightly better separation performance in presence of aqueous solutions  
347 of  $K_3C_6H_5O_7/C_6H_8O_7$ , in agreement with what has been previously demonstrated with other salts [62-  
348 64] and in agreement with the trend observed with the commercial ILs [P<sub>4444</sub>]Br and [N<sub>4444</sub>]Br. Both the



349 IL pairs  $[\text{Bu}_3\text{PC}_4]\text{Br}/[\text{Bu}_3\text{NC}_4]\text{Br}$  and  $[\text{P}_{4444}]\text{Br}/[\text{N}_{4444}]\text{Br}$  comprise the bromide anion, and the  
350 differences in the respective phase diagrams are a result of the charge distribution at the IL cation  
351 central heteroatom which dictates the IL affinity for water [45]. In summary, amongst the AGB-ILs  
352 investigated,  $[\text{MepyrNC}_4]\text{Br}$  displays the lowest capacity to create ABS and requires a higher amount of  
353 citrate-based salt to undergo phase separation, whereas  $[\text{Bu}_3\text{PC}_4]\text{Br}$  is the most effective AGB-IL and  
354 requires the lowest amount of  $\text{K}_3\text{C}_6\text{H}_5\text{O}_7/\text{C}_6\text{H}_8\text{O}_7$  to form ABS. The fitting of the experimental binodal  
355 curves, and the determination of tie-line data and respective length were additionally performed, being  
356 provided in the Supporting Information (Tables S6 and S7). Even though there are 4 ions in solution,  
357 ion exchange is not expected to occur since the probability of different ion pairs to form is significantly  
358 low, as previously confirmed with ABS formed by ionic liquids and strong salting-out salts [65-66],  
359 being this the case of the current work.

360 In summary, it is here shown that AGB-ILs form ABS with  $\text{K}_3\text{C}_6\text{H}_5\text{O}_7/\text{C}_6\text{H}_8\text{O}_7$  at controlled pH  
361 (7.0). In addition, their high thermal stability and low ecotoxicity against *Allvibrio fischeri* support their  
362 further investigation in other ABS to be applied in separation processes of labile biomolecules.

363

#### 364 4. Conclusions

365 In this work, we reported the synthesis and characterization of five new water-soluble analogues of  
366 glycine-betaine-based ionic liquids (AGB-ILs) combined with the bromide anion. Their thermal  
367 properties, namely melting temperature, glass transition temperature and decomposition temperature  
368 were determined and discussed in terms of the IL chemical structure. All synthesized AGB-ILs fit  
369 within the ILs category, with a melting temperature below 100 °C, and present high degradation  
370 temperatures (180-310 °C). Their toxicity against the marine luminescent bacteria *Allvibrio fischeri*  
371 showed that the studied AGB-ILs are harmless or practically harmless and display a lower toxicity of  
372 this marine bacteria than commonly used ILs, such as  $[\text{N}_{4444}]\text{Br}$  and  $[\text{P}_{4444}]\text{Br}$ . Given the AGB-ILs  
373 properties, we studied their potential to create ABS that could be applied in separation processes. The  
374 ABS phase diagrams were determined for systems composed of AGB-IL + water +  $\text{K}_3\text{C}_6\text{H}_5\text{O}_7/\text{C}_6\text{H}_8\text{O}_7$   
375 at pH 7.0 and at 25 °C. The obtained results confirm their high ability to be salted-out by the organic  
376 salt and to form ABS, where more hydrophobic ILs more easily form two-phase systems or require a  
377 lower amount of salt to undergo phase separation in aqueous media. This ability to be salted-out by the  
378 organic salt follows the order  $[\text{Bu}_3\text{PC}_4]\text{Br} > [\text{Bu}_3\text{NC}_4]\text{Br} > [\text{Pr}_3\text{NC}_4]\text{Br} > [\text{Et}_3\text{NC}_4]\text{Br} \approx [\text{MepyrNC}_4]\text{Br}$ .  
379 All the properties shown for the newly reported AGB-ILs are beneficial to develop sustainable and  
380 biocompatible separation processes.

381

#### 382 Acknowledgments

383 This work was developed within the scope of the project CICECO-Aveiro Institute of Materials, FCT  
384 Ref. UID/CTM/50011/2019, financed by national funds through the FCT/MCTES. M. M. Pereira  
385 acknowledges the PhD grant (2740-13-3) and financial support from Coordenação de Aperfeiçoamento  
386 de Pessoal de Nível Superior – Capes and the Short Term Scientific Mission grant COST-STSM-  
387 ECOST-STSM-CM1206–011015-066583. M. G. Freire acknowledges the European Research Council  
388 under the European Union’s Seventh Framework Programme (FP7/2007-2013)/ERC Grant 337753. We  
389 acknowledge D. Harakat for the ESI-MS measurements.

390

## 391 **References**

- 392 [1] A. Schmid, A. Koller, R.G. Mathys, B. Withot, *Extremophiles* 2 (1998) 249-256.
- 393 [2] T.P.T. Pham, C.W. Cho, Y.S. Yun, *Water Research* 44 (2010) 352-372.
- 394 [3] P. Wasserscheid and W. Keim, *Angew. Chem., Int. Ed.* 39 (2000) 3772-3789.
- 395 [4] M.J. Earle, K.R. Seddon, *Pure Appl. Chem.* 72 (2000) 1391-1398.
- 396 [5] J.L. Anderson, J. Ding, T. Welton, D.W. Armstrong, *J. Am. Chem. Soc.* 124 (2002) 14247-  
397 14254.
- 398 [6] J. Dupont, R.F. De Souza, P.A.Z. Suarez, *Chem. Rev.* 102 (2002) 3667-3692).
- 399 [7] A. Jordan, N. Gathergood, *Chem. Soc. Rev.*, 44 (2015) ,8200-8237.
- 400 [8] D.O. Hartmann, C.S. Pereira, *Toxicity of Ionic Liquids: Past, Present, and Future, Ionic Liquids*  
401 *in Lipid Processing and Analysis - Opportunities and Challenges*, 2016, Chapter 13, Pages 403-  
402 421.]
- 403 [9] M. Amde, J.-F. Liu, L. Pang, *Environ. Sci. Technol.* 49 (2015) 12611–12627.
- 404 [10] S.T. Handy, *Chem. Eur. J.* 9 (2003) 2938-2944.
- 405 [11] D.-J. Tao, Z. Cheng, F.-F. Chen, Z.-M. Li, N. Hu, X.-S. Chen, *J. Chem. Eng. Data* 58 (2013),  
406 1542–1548.
- 407 [12] N. Muhammad, M.I. Hossain, Z. Man, M. El-Harbawi, M. A. Bustam, Y. Ab. Noaman, N.B.M.  
408 Alitheen, M.K. Ng, G. Hefter, C.-Y. Yin, *J. Chem. Eng. Data* 57 (2012) 2191–2196.
- 409 [13] R. Vijayaraghavan, B.C. Thompson, D.R. MacFarlane, R. Kumar, M. Surianarayanan, S.  
410 Aishwarya, P.K. Sehga, *Chem. Commun.* 46 (2010) 294–296.
- 411 [14] Y-X. An, M.-H. Zong, H. Wu, N. Li, *Bioresour. Technol.* 192 (2015) 165–171.
- 412 [15] S. Yuan, Y. Chen, X. Ji, Z. Yang, X. Lu, *Fluid Phase Equilib.* 445 (2017) 14-24.
- 413 [16] P. Moriel, E. J. García-Suárez, M. Martínez, A. B. García, M. A. Montes-Morán, V. Calvino-  
414 Casilda, M. A. Bañares, *Tetrahedron Lett.* 51 (2010) 4877–4881.
- 415 [17] S. Hu, T. Jiang, Z. Zhang, A. Zhu, B. Han, J. Song, Y. Xie, W. Li , *Tetrahedron Lett.* 48 (2007)  
416 5613–5617.



- 417 [18] D.-J. Tao, Z. Cheng, F.-F. Chen, Z.-M. Li, N. Hu, X.-S. Chen, *J. Chem. Eng. Data* 58 (2013) 58  
418 1542–1548.
- 419 [19] X.-D. Hou, T.J. Smith, N. Li, M.-H. Zong, *Biotechnol. Bioeng.* 109 (2012) 2484-2493.
- 420 [20] Poletti, C. Chiappe, L. Lay, D. Pieraccini, L. Polito, G. Russo, *Green Chem.* 9 (2007) 337–341.
- 421 [21] A. K. Jha, N. Jain, *Tetrahedron Lett.* 54 (2013) 4738–4741.
- 422 [22] Y. De Gaetano, A. Mohamadou, S. Boudesocque, J. Hubert, R. Plantier-Royon, L. Dupont, J.  
423 *Mol Liq.* 207 (2015) 60-66.
- 424 [23] A. Messadi, A. Mohamadou, S. Boudesocque, L. Dupont, P. Fricoteaux, A. Nguyen-Van-Nhien,  
425 M. Courty, *J. Mol Liq.* 184 (2013) 68-72.
- 426 [24] Y. De Gaetano, J. Hubert, A. Mohamadou, S. Boudesocque, R. Plantier-Royon, J.H. Renault, L.  
427 Dupont, *Chem. Eng. J.* 285 (2016) 596-604.
- 428 [25] A. Messadi, A. Mohamadou, S. Boudesocque, L. Dupont, E. Guillon, *Sep. Purif. Technol.* 107  
429 (2013) 172-178. 31.
- 430 [26] Y. Zhou, S. Boudesocque, A. Mohamadou, L. Dupont, *Sep. Sci. Technol.* 50 (2015) 38-44.
- 431 [27] S. Boudesocque, A. Mohamadou, L. Dupont, *New J. Chem.*, 38 (2014) 5573-5581.
- 432 [28] A. M. Ferreira, E. S. Morais, A. C. Leite, A. Mohamadou, B. Holmbom, T. Holmbom, B. M.  
433 Neves, J. A. P. Coutinho, M. G. Freire, A. J. D. Silvestre, *Green Chem.* 19 (2017) 2626-2635.
- 434 [29] D. Coleman and N. Gathergood, *Chem. Soc. Rev.* 39 (2010) 600–637
- 435 [30] A. Sakamoto, N. Murata, *Plant, Cell Environ.* 25 (2002) 163-171.
- 436 [31] M. Ashraf, M.R. Foolad, *Environ. Exp. Bot.* 59 (2007) 206-216.
- 437 [32] J. R. Hoffman, N. A. Ratamesh, J. Kang, S. L. Rashti and A. D. Faigenbaum, *J. Int. Soc. Sports*  
438 *Nutr.* 6 (2009) 7-7.
- 439 [33] Z. F. Nsimba, M. Paquot, L. G. Mvumbi and M. Deleu, *Biotechnol. Agron. Soc. Environ.* 14  
440 (2010) 737-748.
- 441 [34] S. M. Steinberg, E. J. Poziomek, W. H. Engelmann and K. R. Rogers, *Chemosphere* 30 (1995)  
442 155–2197.
- 443 [35] M. Corporation, Microtox<sup>®</sup> manual—a toxicity testing hand-book, Microbics Corporation, 1992,  
444 Carlsbad, 1–5.
- 445 [36] S.P.M. Ventura, A.M.M. Gonçalves, F. Gonçalves, J.A.P. Coutinho, *Aquat. Toxicol.* 96 (2010)  
446 290-297.
- 447 [37] B.T. Johnson, Microtox acute toxicity test in C. blaise J.-F. Férard (Eds), *Small-scale Freshwater*  
448 *toxicity Investigation*, Springer, Netherlands, pp. 69-105.
- 449 [38] A. Environmental, Carlsbad CA, USA, 1998.
- 450 [39] Azur Environmental, 1998. Azur Environmental, Microtox Manual. [www.azueenv.com](http://www.azueenv.com).

- 451 [40] C.M.S.S. Neves, S.P.M. Ventura, M.G. Freire, I.M. Marrucho, J.A.P. Coutinho, *J. Phys. Chem.*  
452 *B* 113 (2009) 5194–5199.
- 453 [41] S.P.M. Ventura, S.G. Sousa, L.S. Serafim, Á.S. Lima, M.G. Freire, J.A.P. Coutinho, *J. Chem.*  
454 *Eng. Data* 56 (2011) 4253–4260.
- 455 [42] H. Passos, A.R. Ferreira, A.F.M. Cláudio, J.A.P. Coutinho, M.G. Freire, *Biochem. Eng. J.*, 67  
456 (2012) 68-76.
- 457 [43] J.C. Merchuk, B.A. Andrews, J.A. Asenjo, *J Chromatogr., B: Biomed. Sci. Appl.* 711 (1998)  
458 285-293.
- 459 [44] J. D. Holbrey and K. R. Seddon, *J. Chem. Soc., Dalton Trans.* (1999) 2133–2139.
- 460 [45] P.J. Carvalho, S.P.M. Ventura, M.L.S. Batista, B. Schröder, F. Gonçalves, J. Esperança, F.  
461 Mutelet, J.A.P. Coutinho *J. Chem. Phys.* 140 (2014) 064505.
- 462 [46] W. Kauzmann, *Chem. Rev.* 43 (1948) 219–256.
- 463 [47] R. G. Beaman, *Polymer Sci.* 9 (1952) 470–472.
- 464 [48] J. Kagimoto, K. Fukumoto, H. Ohno *Chem. Commun.* 2006, 2254–2256
- 465 [49] C. Maton, N. De Vos, C. V. Stevens, *Chem. Soc. Rev.* 42 (2013) 5963-5977.
- 466 [50] K. Tsunashima, S. Kodama, M. Sugiya, Y. Kunugi, *Electrochim. Acta* 56 (2010) 762-766.
- 467 [51] S.P.M. Ventura, C.S. Marques, A.A. Rosatella, C.A.M. Alfonso, F. Gonçalves, J.P.A. Coutinho,  
468 *Ecotoxicol. Environ. Saf.* 76 (2012) 162-168.
- 469 [52] M. M. Pereira, J. Gomes, M. R. Almeida, J. A. P. Coutinho, A. Mohamadou, M. G. Freire,  
470 *Biotechnol. Prog.* **2018**, 34, 1205-1212.
- 471 [53] S. Stolte, M. Matzke, J. Arning, A. Boschen, W.R. Pitner, U. Welz-Biermann, B. Jastorff, J.  
472 Ranke, *Green Chem.* 9 (2007) 1170-1179
- 473 [54] S.P.M. Ventura, A.M.M. Gonçalves, T. Sintra, J. Pereira, F. Gonçalves, J.A.P. Coutinho,  
474 *Ecotoxicology* 22 (2013) 1-12.
- 475 [55] D.J. Couling, R.J. Bernot, K.M. Docherty, J.K. Dixon, E.J. Maginn, *Green Chem.* 8 (2006) 82-  
476 90.
- 477 [56] D.R.M. Passino, S.B. Smith, *Environ. Toxicol. Chem.* 6 (1987) 901-907.
- 478 [57] F.A. e Silva, T. Sintra, S.P.M. Ventura, J.A.P. Coutinho, *Sep. Purif. Technol.* 122 (2014) 315–  
479 322.
- 480 [58] M.M. Pereira, S.N. Pedro, M.V. Quental, Á. S. Lima, J.A.P. Coutinho, M. G. Freire, J.  
481 *Biotechnol.* 206 (2015) 17–25.
- 482 [59] C.M.S.S. Neves, S.P.M. Ventura, M.G. Freire, I.M. Marrucho, J.A.P. Coutinho, *J. Phys; Chem.*  
483 *B* 113 (2009) 5194-5199.
- 484 [60] A.F.M. Claudio, A.M. Ferreira, S. Shahriari, M.G. Freire, J.A.P. Coutinho, *J. Phys. Chem. B*  
485 115 (2011) 11145-11153.

- 486 [61] S.P.M. Ventura, S.G. Sousa, L.S. Serafim, A.S. Lima, M.G. Freire, J.A.P. Coutinho, J. Chem  
487 Eng. Data 56 (2011) 4253-4260.
- 488 [62] L.S. Louros, A.F.M. Cláudio, C.M.S.S. Neves, M. G. Freire, I.M. Marrucho, P. Jérôme, J.A.P.  
489 Coutinho, Int. J. Mol. Sci. 11 (2010) 1777-1791.
- 490 [63] M.M. Pereira, S.N. Pedro, M.V. Quental, Á.S. Lima, J.A.P. Coutinho, M .G. Freire, J.  
491 Biotechnol. 206 (2015) 17-25.
- 492 [64] T.E. Sintra, R. Cruz, S.P.M. Ventura, J.A.P. Coutinho, J. Chem. Thermodyn. 77 (2014) 206-213.
- 493 [65] C.M.S.S. Neves, M.G. Freire, J.A.P. Coutinho, RSC Adv. 2 (2012) 10882-10890.  
494
- 495 [66] N.J. Bridges, K.E. Gutowski, R.D. Rogers, Green Chem. 9 (2007) 177-183.

**Fig. 1.** Synthetic route of AGB-ILs.

**Fig. 2.** TGA profile for bromide based AGB-ILs.

**Fig. 3.** Ternary phase diagrams, in an orthogonal representation, for the systems composed of IL + water +  $K_3C_6H_5O_7/C_6H_8O_7$  buffered at pH = 7.0 and at 25°C: [MepyrNC<sub>4</sub>]Br (▲); [Et□NC<sub>4</sub>]Br (●); [Pr□NC<sub>4</sub>]Br (■); [Bu□NC□]Br (◆); [Bu<sub>3</sub>PC<sub>4</sub>]Br (●), [N<sub>4444</sub>]Br (▲) [57]; [P<sub>4444</sub>]Br (■) [58].

497

**Table 1**

498 Name, CAS-number, molecular weight, purity and suppliers of applied chemicals.  
499

**Table 2**

500 Name, abbreviation, chemical structure and molecular weight of the synthesized AGB-ILs, and of two  
501 commercial ILs investigated for comparison purposes.

**Table 3**

Melting ( $T_m$ ), glass transition ( $T_g$ ) and decomposition ( $T_{dc}$ ) temperatures for the synthesized AGB-ILs.

**Table 4**

Microtox<sup>®</sup> EC<sub>50</sub> values (mg.L<sup>-1</sup>) for *Allvibrio fischeri* after 5, 15 and 30 min of exposure to aqueous solutions of AGB-ILs and of two commercial ILs [51, 52] with the respective 95% confidence limits (in brackets).